

Abstract

In this work we study the Zeeman effect on stratospheric O₂ using ground-based microwave radiometer measurements. The interaction of the Earth magnetic field with the oxygen dipole leads to a splitting of O₂ energy states which polarizes the emission spectra. A special campaign was carried out in order to measure this effect in the oxygen emission line centered at 53.07 GHz. Both a fixed and a rotating mirror were incorporated to the TEMPERA (TEMPERature RAdiometer) radiometer in order to be able to measure under different observational angles. This new configuration allowed us to change the angle between the observational path and the Earth magnetic field direction. Moreover, a high resolution spectrometer (1 kHz) was used in order to measure for the first time the Zeeman effect in the main isotopologue of oxygen from ground-based microwave measurements. The measured spectra showed a clear polarized signature when the observational angles were changed evidencing the Zeeman effect in the oxygen molecule. In addition, simulations carried out with the Atmospheric Radiative Transfer Simulator (ARTS) allowed us to verify the microwave measurements showing a very good agreement between model and measurements. The results suggest some interesting new aspects for research of the upper atmosphere.

1 Introduction

The Zeeman effect is a phenomenon which occurs when an external magnetic field interacts with a molecule or an atom of total electron spin different from zero. Such an interaction will split an original energy level into several sub-levels (Lenoir, 1967). In the atmosphere, oxygen is an abundant molecule which in its ground electronic state has a permanent magnetic dipole moment coming from two parallel electron spins. The interaction of the magnetic dipole moment with the Earth magnetic field leads to a Zeeman splitting of the O₂ rotational transitions. In this state each rotational level, with quantum number N is split into 3 levels of total quantum number $J(J_{\pm})$ following

Zeeman effect measurements in atmospheric O₂

F. Navas-Guzmán et al.

Title Page

Abstract

Introduction

Conclusions

References

Tables

Figures



Back

Close

Full Screen / Esc

Printer-friendly Version

Interactive Discussion



a comparison of other radiative transfer model with measurements of the 118 GHz oxygen line from the Microwave Limb Sounder (MLS) on board of Aura spacecraft.

In this work we present an experiment where the Zeeman broadening of the oxygen emission line at 53.0669 GHz is observed for the first time using a ground-based microwave radiometer. The measurements were possible using a Fast Fourier Transform (FFT) spectrometer with 1 GHz of bandwidth to measure the whole oxygen emission line centered at 53.07 GHz and a narrow spectrometer (4 MHz) to measure the center of the line with a very high resolution (1 kHz). These measurements have been compared to a model which includes the Zeeman-splitting effect. The incorporation of this effect to the forward model will allow to extend the temperature retrievals beyond 50 km. This improvement in the forward model will be very useful for the assimilation of brightness temperatures in numerical weather prediction (NWP) models.

The paper is organized as follows: in Sect. 2, the instrumentation and the measurements are briefly outlined. The Zeeman effect theory and the modeling are presented in Sect. 3. Section 4 presents the results of this study. Firstly the simulations using a model are addressed and secondly the tropospheric correction performed to the radiometer measurements and the results obtained during this campaign are presented. Finally, the conclusions are given in Sect. 5.

2 Instrumentation and measurements

The TEMPERA radiometer is a microwave radiometer that provides temperature profiles from ground to around 50 km (Stähli et al., 2013). This is the first microwave radiometer that measures temperature in the troposphere and stratosphere at the same time. The instrument is a heterodyne receiver at a frequency range of 51–57 GHz. Figure 1 shows a picture of TEMPERA which is operated in a temperature-stabilized laboratory at the ExWi Building of the University of Bern (Bern, Switzerland; 575 m above sea level; 46.95° N, 7.44° E). In this lab a styrofoam window allows views of the atmosphere over the zenith angle (z_a) range from 30 to 70°. The instrument mainly

Zeeman effect measurements in atmospheric O₂

F. Navas-Guzmán et al.

Title Page

Abstract

Introduction

Conclusions

References

Tables

Figures



Back

Close

Full Screen / Esc

Printer-friendly Version

Interactive Discussion



olution of 1 kHz. An example of a monthly mean brightness temperature spectrum centered at 53.07 GHz measured with the SDR spectrometer is shown in Fig. 2b.

Moreover, a set of two auxiliary mirrors were installed on the roof of the ExWi Building in the University of Bern (Fig. 3). A rotating mirror allows to observe the atmosphere under different azimuth angles and with a fixed elevation angle, while the fixed mirror directs the radiation from the rotating mirror into TEMPERA radiometer. The main goal of using these auxiliary mirrors is to measure the Zeeman-broadened oxygen line under different angles relative to the Earth magnetic field.

A special campaign was carried out in Autumn of 2013 in order to detect the Zeeman effect with TEMPERA. Three months of measurements (September–November 2013) were performed using these auxiliary mirrors and the SDR spectrometer. A special measurement cycle was designed for TEMPERA during this period. Periodic cycles of almost 5 min were performed. This whole cycle consisted of 13 sub-cycles where each one starts with a hot load calibration in combination with a noise diode for 10 s followed by other 10 s of atmospheric measurements in one azimuth direction. A total of 13 azimuth angles were scanned ranging from 71.5 to 191° in steps of 10° during the whole cycle. The elevation angle was fixed at 60° during all the measurements since it was found as the angle in which the intensity of the emission lines was highest (Stähli et al., 2013).

3 Zeeman effect theory and modeling

3.1 Theory

The Zeeman effect (Zeeman, 1897) occurs because the spin of unpaired electrons couples to the external magnetic field, changing the internal energy of the molecule. A transition between two of these altered energy levels can change the frequency dependence of the absorption spectrum. The Zeeman energy change is calculated by

$$\Delta E = -g\mu_0 M |H|, \quad (1)$$

Zeeman effect measurements in atmospheric O₂

F. Navas-Guzmán et al.

Title Page

Abstract

Introduction

Conclusions

References

Tables

Figures



Back

Close

Full Screen / Esc

Printer-friendly Version

Interactive Discussion



among other new features, a module that calculates the Zeeman effect presented by Larsson et al. (2014).

In short, ARTS calculates each of the three polarization components individually before adding their absorption contributions to a Stokes vector propagation matrix. The polarization of the radiation is internally kept in a universal coordinate system defined by the sensor through all of the propagation. The line shape should return both its imaginary and real part to account for dispersion-caused polarization rotation. The input magnetic field is either static or three 3-D-gridded fields, one field for each coordinate: x , y , and z . This propagation matrix is then sent to the radiative transfer calculator, which solves the vector radiative transfer equation (as in e.g. del Toro Iniesta, 2003)

$$\frac{dI}{dr} = -\mathbf{K}(I - \mathbf{B}), \quad (2)$$

where I is the Stokes vector, r is the path vector, \mathbf{K} is the propagation matrix, and \mathbf{B} is the Stokes version of Planck's function for blackbody radiation. For details on the ARTS Zeeman effect module see Larsson et al. (2014).

The calculated relative Zeeman pattern for the line measured by TEMPERA can be found in Fig. 4. This otherwise singular line is split into 159 Zeeman lines; 53 for each polarization component. The plot has been renormalized for readability. The strongest split line accounts for less than 1.5% of the original strength of the line, the maximum splitting from the central line is $\sim 27.99 \text{ kHz } (\mu\text{T})^{-1}$, and the splitting between the individual lines is about $1.08 \text{ kHz } (\mu\text{T})^{-1}$ within a component. The last number is significantly small. The thermal broadening in the stratosphere is under normal conditions larger than the magnetic line splitting above Bern, so individual Zeeman lines cannot be discerned from the overall shape.

Zeeman effect measurements in atmospheric O₂

F. Navas-Guzmán et al.

Title Page

Abstract

Introduction

Conclusions

References

Tables

Figures



Back

Close

Full Screen / Esc

Printer-friendly Version

Interactive Discussion



4 Results

4.1 Brightness temperature simulations incorporating the Zeeman effect

Brightness temperature spectra have been simulated using the ARTS model which has been described in the previous section. ARTS was set with all the information about instrumental aspects and location of TEMPERA in order to simulate the same measurement conditions. The brightness temperature was calculated for thirteen azimuth angles ($71.5^\circ : 10^\circ : 191.5^\circ$), a fixed elevation angle (60°) and simulating the atmospheric conditions of 15 October 2013 (Fig. 5). The altitude of the platform was set at 12 km in order to avoid any tropospheric effect in the spectra. On 15 October 2013, the total intensity of the magnetic field over Bern at the altitude of 50 km was 46 547 nT with a declination of $1^\circ 21' 44''$ and an inclination of $62^\circ 46' 16''$ (www.ngdc.noaa.gov/geomag/magfield.shtml). Figure 5a shows the calculated brightness temperature spectra for a linear horizontal polarization of the oxygen emission line centered at 53.07 GHz in a range of 5 MHz. From these simulations we can observe that the spectra are almost identical for most of the frequency range plotted here and differences are only observed in the central part when the observational azimuth angle is changed. In the narrow central frequency range we can observe that both the shape and the intensity of the spectra change for the different observations. For the higher azimuth angles the brightness temperature spectra are lower and the shape is flatter while for lower angles the spectra are higher and the shape is less flat. The maximum difference in brightness temperature between the most intensive spectrum (91.5°) and the least intensive (191.5°) is 2.5 K. Figure 5b shows linear vertical polarization. We observe a similar pattern for linear vertical polarization as we do for linear horizontal polarization, with the peak strength of the signal changing mostly in the center of the line as a function of the azimuthal angle. However, the change is much smaller for linear vertical polarization, which only has a maximum difference of 1 K between the most and least intense spectra. Also, the change with azimuthal angle is inverted compared to linear horizontal polarization. For the linear vertical polarization the most intensive

Title Page

Abstract

Introduction

Conclusions

References

Tables

Figures



Back

Close

Full Screen / Esc

Printer-friendly Version

Interactive Discussion



spectrum corresponds to the observational angle of 181.5° while the least intensive corresponds to 91.5° . This behaviour is clearly associated with the polarized nature of the Zeeman effect, since the polarized state of the observed radiation changes when the angle between the propagation path and the direction of the Earth magnetic field is varied.

The brightness temperature has also been simulated without considering the Zeeman effect in the ARTS model. These simulations correspond to the dashed lines shown in Fig. 5. We found that when the Zeeman module is not active there is no difference in the spectra for difference observational angles. Moreover, the spectrum presents higher brightness temperature values and it does not show any broadening in the center of the oxygen emission line.

In order to compare the simulated spectra from ARTS with the measurements, the effects of the different optical components of TEMPERA on the polarization state of the radiation, as well as the vertically polarized observing antenna, have to be considered. A full characterization of the polarization state of the radiation can be done by means of the Stokes vector, \mathbf{s} , which is defined as

$$\mathbf{s} = \begin{bmatrix} I \\ Q \\ U \\ V \end{bmatrix} = \frac{1}{2} \sqrt{\frac{\varepsilon}{\mu}} \begin{bmatrix} \langle E_v E_v^* + E_h E_h^* \rangle \\ \langle E_v E_v^* - E_h E_h^* \rangle \\ \langle E_v E_h^* - E_h E_v^* \rangle \\ \langle E_h E_v^* - E_v E_h^* \rangle \end{bmatrix} \quad (3)$$

where ε and μ are the electric and magnetic constants, respectively, $\langle \cdot \rangle$ indicates time average and E_v and E_h are the complex amplitudes for vertical and horizontal polarization. The first Stokes component (I) is the total intensity, the second component (Q) is the difference between vertical and horizontal polarization, and the last two components, U and V , correspond to linear $\pm 45^\circ$ and circular polarization, respectively. The Stokes components are converted to brightness temperature by inverting the Planck function (Eriksson et al., 2011), this new Stokes vector of brightness temperatures is denoted as \mathbf{s}' .

Zeeman effect measurements in atmospheric O₂

F. Navas-Guzmán et al.

Title Page

Abstract

Introduction

Conclusions

References

Tables

Figures



Back

Close

Full Screen / Esc

Printer-friendly Version

Interactive Discussion



The calculus of the measured brightness temperature (T_b^p) considering the sensor polarization response can be expressed as (cf. Eriksson et al., 2011, Eq. 19)

$$T_b^p = \boldsymbol{p} \boldsymbol{s}' \quad (4)$$

where \boldsymbol{p} is a row vector of length 4 which describes the sensor polarization response. In the case of TEMPERA, whose antenna is vertically polarized, the vector \boldsymbol{p} is [1 1 0 0].

The rotation of the Stokes reference frame due to the reflection in the different mirrors and also to the rotation of the external mirror is considered using a transformation matrix $\mathbf{L}(\chi)$, which allows to obtain a consistent definition between the polarization directions for atmospheric radiation and sensor response. This matrix is defined as (Liou, 2002):

$$\mathbf{L}(\chi) = \begin{bmatrix} 1 & 0 & 0 & 0 \\ 0 & \cos 2\chi & \sin 2\chi & 0 \\ 0 & -\sin 2\chi & \cos 2\chi & 0 \\ 0 & 0 & 0 & 1 \end{bmatrix} \quad (5)$$

The rotational angle (χ) has been calculated using the GRASP software package (www.ticra.com/products/software/grasp). This software package allows design and analysis of complex reflector elements using physical optics, physical theory of diffraction and the method of moments. Figure 6 shows the setup of this simulation, where we can see the different TEMPERA components (horn antenna, parabolic mirror and the two auxiliary mirrors, the fixed and the rotating mirror) and the ray tracing of an electric field which is propagated from the antenna to the atmosphere. The calculated angle χ can be expressed as $\chi = \varphi + \varphi_{\text{offset}}$, where φ is the observational azimuth angle defined in our experiments ($\varphi = 71.5^\circ : 10^\circ : 191.5^\circ$) and φ_{offset} is 141.5° . Once the sensor polarization response and the rotation of the polarized radiation have been characterized the effective brightness temperature can be calculated as (Eriksson et al., 2006)

$$T_b^p = \boldsymbol{p} \mathbf{L}(\chi) \boldsymbol{s}' \quad (6)$$

Zeeman effect measurements in atmospheric O₂

F. Navas-Guzmán et al.

Title Page

Abstract

Introduction

Conclusions

References

Tables

Figures



Back

Close

Full Screen / Esc

Printer-friendly Version

Interactive Discussion



Zeeman effect measurements in atmospheric O₂

F. Navas-Guzmán et al.

Title Page

Abstract

Introduction

Conclusions

References

Tables

Figures

◀

▶

◀

▶

Back

Close

Full Screen / Esc

Printer-friendly Version

Interactive Discussion



Figure 7 shows the effective brightness temperature spectra calculated for the case simulated in ARTS (15 October 2013) in Fig. 5. For these spectra we can appreciate again the same pattern as in the ARTS simulations, with almost the same intensity on the wings of the oxygen emission line and some differences in the central frequencies when the azimuth angle is changed. The highest brightness temperature is found at 71.5° while the lowest is found at 191.5°. The latter position corresponds to the maximum broadening found when the direction of observation is almost antiparallel to the direction South–North. The maximum difference between the most and the least intense spectra is 2.5 K.

In order to study the difference in the broadening of each azimuth observational spectrum due to the Zeeman effect, we have calculated the ratio between each spectrum and the averaged spectrum from all the observational angles. Figure 8 shows these ratios for the different azimuth angles. Azimuthal behaviour with a ratio below unity in the center of the line also has a ratio above unity in the wings, which means that the line experienced more than averaged broadening. The opposite is also true, azimuthal behavior with values above unity in the center means less than averaged broadening. The different ratios show a clear azimuth dependence showing that the highest broadening is found when the azimuth angle is 191.5° while the smaller broadening is found at 71.5°.

4.2 Tropospheric correction of SDR spectrometer

A ground-based microwave radiometer measures a superposition of emission and absorption of radiation at different altitudes. The received intensity at ground level can be expressed in the Rayleigh–Jeans limit ($h\nu \ll kT$) as a function of the brightness temperature. In these conditions the radiative transfer equation is given by

$$T_b(\nu, z_0) = T_0 e^{-\tau(\nu, z_1)} + \int_{z_0}^{z_1} T(z) e^{-\tau(\nu, z)} \alpha(\nu, z) dz \quad (7)$$

where T_b is the brightness temperature at frequency ν , T_0 is the brightness temperature of the cosmic background radiation, $T(z)$ is the physical temperature at height z , z_0 is the Earth surface, z_1 is the upper boundary in the atmosphere, α is the absorption coefficient and τ is the opacity. The opacity is defined as

$$\tau(\nu, z) = \int_{z_0}^z \alpha(\nu, z') dz' \quad (8)$$

The contribution of the troposphere to the brightness temperature measured with a microwave radiometer at ground level is very important and it could be very different depending on the observational direction or on the period of measurements. After oxygen, water vapour and liquid water (clouds) are the most important components in the atmosphere whose emissions have relevance in the microwave spectrum. It is very important to correct our measurements for any tropospheric effect in order to ensure that the changes observed in our measurements for different observational directions come from the stratosphere (Zeeman effect) and not from the troposphere.

In order to correct our measurements for tropospheric effects, the microwave radiative transfer equation is rewritten as

$$T_b(z_0) = T_b(z_{\text{trop}})e^{-\tau} + T_{\text{trop}}(1 - e^{-\tau}) \quad (9)$$

where $T_b(z_{\text{trop}})$ is the brightness temperature as observed from the tropopause, τ is the tropospheric zenith opacity and T_{trop} is the effective temperature of the troposphere.

From this equation the opacity can be calculated as

$$\tau = -\ln \left(\frac{T_{\text{trop}} - T_b(z_0)}{T_{\text{trop}} - T_b(z_{\text{trop}})} \right) \quad (10)$$

Since the atmospheric opacity is dominated by the contribution from the troposphere, the cosmic background radiation, T_{bg} , is in practice used instead of $T_b(z_{\text{trop}})$ in Eq. (10).

Zeeman effect measurements in atmospheric O₂

F. Navas-Guzmán et al.

Title Page

Abstract

Introduction

Conclusions

References

Tables

Figures



Back

Close

Full Screen / Esc

Printer-friendly Version

Interactive Discussion



This means that the calculated τ actually is approximately the total atmospheric opacity and hence includes the minor contribution from altitudes above the troposphere (e.g. absorption by stratospheric O₂ and H₂O) (Forkman et al., 2012).

T_{trop} has been estimated using a linear model between the weighted tropospheric temperature and the ground temperature (Ingold et al., 1998). The weighted tropospheric temperature was calculated using radiosonde measurements. Radiosondes are launched twice a day at the aerological station of MeteoSwiss in Payerne (40 km W of Bern). One year of radiosonde data were used and the linear fit found between T_{trop} at 53 GHz and the ground temperature T_{z_0} was $T_{\text{trop}} = 0.8159T_{z_0} + 47.21$ K. The constant term T_{bg} is independent of frequency and has a value of 2.7 K (Gush et al., 1990). The term $T_{\text{b}}(z_0)$ is measured using the wings of the oxygen emission line centered at 53.07 GHz for every azimuth angle. The simultaneous measurements performed with the FFT spectrometer allow us to measure in the wings of the oxygen emission line, where most of the contribution to the brightness temperature comes from the troposphere. In the frequency range of interest, the tropospheric attenuation increases with increasing frequency. In order to account for this, we determine the correction factor at each frequency using a linear fit between the frequency ranges highlighted in red in Fig. 9.

Once all the terms are calculated the brightness temperature corrected for tropospheric effects can be obtained as:

$$T_{\text{b}}(z_{\text{trop}}) = \frac{T_{\text{b}}(z_0) - T_{\text{trop}}(1 - e^{-\tau})}{e^{-\tau}}. \quad (11)$$

It is interesting to note that for the correction presented in this section we have used the scalar radiative transfer equation, since this tropospheric correction is independent of polarization state. This assumption is valid if scattering can be neglected, which should hold in the absence of strong precipitation.

Zeeman effect measurements in atmospheric O₂

F. Navas-Guzmán et al.

Title Page

Abstract

Introduction

Conclusions

References

Tables

Figures

⏪

⏩

◀

▶

Back

Close

Full Screen / Esc

Printer-friendly Version

Interactive Discussion



4.3 Stratospheric brightness temperature measurements

As already described in Sect. 2, a special campaign of microwave radiometer measurements has been performed for three months in autumn 2013 in the ExWi Building of University of Bern. During this campaign, TEMPERA was set with a special configuration in order to be able to observe the Zeeman effect from ground-based measurements. Radiometer measurements in different azimuth angles (13 angles) were carried out in order to scan the atmosphere under different angles between the propagation path and the local Earth magnetic field. Figure 10 shows mean monthly brightness temperature spectra obtained for different azimuth angles in October 2013. All the measurements were corrected for tropospheric effects following the procedure described in the previous section. Figure 10a shows the whole range (4 MHz) measured with the SDR spectrometer. From this plot we observe that the mean spectra for the different azimuth angles show almost identical values outside of the narrow central region. However, differences in the intensity and in the shape are observed in the very narrow range centered on 53.07 GHz. Figure 10b shows a zoom of the spectra in the central frequencies for some selected azimuth angles. We can observe that for higher azimuth angles the spectra show lower values of brightness temperature and flatter shapes in the central frequency range (± 0.5 MHz) while higher brightness temperature and less flat shapes are observed in lower azimuth angles.

These results are in good agreement with the simulations performed including the Zeeman effect with ARTS (Sect. 4.1). In order to compare in a more quantitative way the measurements with the model we have compared the ratio between the maximum mean brightness temperature of each spectrum and the mean value for all the spectra at the central frequencies (range of 0.5 MHz). Figure 11 shows these ratios calculated with the ARTS model simulating the conditions of 15 October 2013 and the ones obtained from the mean monthly spectra (October 2013) measured by TEMPERA. We can observe, that in general, there is a very good agreement between the measurements and the model. Both simulations and measurements show higher ratio values

AMTD

8, 1–32, 2015

Zeeman effect measurements in atmospheric O₂

F. Navas-Guzmán et al.

Title Page

Abstract

Introduction

Conclusions

References

Tables

Figures



Back

Close

Full Screen / Esc

Printer-friendly Version

Interactive Discussion



Zeeman effect measurements in atmospheric O₂

F. Navas-Guzmán et al.

Title Page

Abstract

Introduction

Conclusions

References

Tables

Figures



Back

Close

Full Screen / Esc

Printer-friendly Version

Interactive Discussion



Gautier, D.: Influence du champ magnetique terrestre sur le transfert du rayonnement millimetrique dans l'oxygene moleculaire de l'atmosphere, *Ann. Geophys.*, 23, 535–568, 1967, <http://www.ann-geophys.net/23/535/1967/>. 3

Gush, H. P., Halpern, M., and Wishnow, E. H.: Rocket measurement of the cosmic-background-radiation mm-wave spectrum, *Phys. Rev. Lett.*, 65, 537, doi:10.1103/PhysRevLett.65.537, 1990. 14

Han, Y., Weng, F., Liu, Q., and van Delst, P.: A fast radiative transfer model for SS-MIS upper atmosphere sounding channels, *J. Geophys. Res.-Atmos.*, 112, D11121, doi:10.1029/2006JD008208, 2007. 3

Han, Y., van Delst, P., and Weng, F.: An improved fast radiative transfer model for special sensor microwave imager/sounder upper atmosphere sounding channels, *J. Geophys. Res.-Atmos.*, 115, D15109, doi:10.1029/2010JD013878, 2010. 3

Hartmann, G. K., Degenhardt, W., Richards, M. L., Liebe, H. J., Hufford, G. A., Cotton, M. G., Bevilacqua, R. M., Olivero, J. J., Kämpfer, N., and Langen, J.: Zeeman splitting of the 61 gigahertz oxygen (O₂) line in the mesosphere, *Geophys. Res. Lett.*, 23, 2329–2332, 1996. 3

Ingold, T., Peter, R., and Kämpfer, N.: Weighted mean tropospheric temperature and transmittance determination at millimeter-wave frequencies for ground-based applications, *Radio Sci.*, 33, 905–918, 1998. 14

Larsson, R., Buehler, S. A., Eriksson, P., and Mendrok, J.: A treatment of the Zeeman effect using Stokes formalism and its implementation in the Atmospheric Radiative Transfer Simulator (ARTS), *J. Quant. Spectrosc. Ra.*, 133, 445–453, 2014. 8

Lenoir, W. B.: Propagation of partially polarized waves in a slightly anisotropic medium, *J. Appl. Phys.*, 38, 5283–5290, 1967. 2, 3

Lenoir, W. B.: Microwave spectrum of molecular oxygen in the mesosphere, *J. Geophys. Res.*, 73, 361–376, 1968. 3

Liou, K. N.: *An Introduction to Atmospheric Radiation*, 2nd Edn., Academic Press, London, 2002. 11

Navas-Guzmán, F., Stähli, O., and Kämpfer, N.: An integrated approach toward the incorporation of clouds in the temperature retrievals from microwave measurements, *Atmos. Meas. Tech.*, 7, 1619–1628, doi:10.5194/amt-7-1619-2014, 2014. 5

Pardo, J. R., Pagani, L., Gerin, M., and Prigent, C.: Evidence of the Zeeman splitting in the 2₁ [rarr] 0₁ rotational transition of the atmospheric ¹⁶O ¹⁸O molecule from ground-based measurements, *J. Quant. Spectrosc. Ra.*, 54, 931–943, 1995. 3

Zeeman effect measurements in atmospheric O₂

F. Navas-Guzmán et al.

Title Page

Abstract

Introduction

Conclusions

References

Tables

Figures



Back

Close

Full Screen / Esc

Printer-friendly Version

Interactive Discussion



Rosenkranz, P. W.: Absorption of microwaves by atmospheric gases, in: *Atmospheric Remote Sensing by Microwave Radiometry*, edited by: Janssen, M. A., Wiley, J., and Hoboken, N. J., 1993. 3

Rosenkranz, P. W. and Staelin, D. H.: Polarized thermal microwave emission from oxygen in the mesosphere, *Radio Sci.*, 23, 721–729, 1988. 3

Rothman, L. S., Gordon, I. E., Babikov, Y., Barbe, A., Chris Benner, D., Bernath, P. F., Birk, M., Bizzocchi, L., Boudon, V., Brown, L. R., Campargue, A., Chance, K., Cohen, E. A., Coudert, L. H., Devi, V. M., Drouin, B. J., Fayt, A., Flaud, J.-M., Gamache, R. R., Harrison, J. J., Hartmann, J.-M., Hill, C., Hodges, J. T., Jacquemart, D., Jolly, A., Lamouroux, J., Le Roy, R., J., Li, G., Long, D. A., Lyulin, O. M., Mackie, C. J., Massie, S. T., Mikhailenko, S., Müller, H. S. P., Naumenko, O. V., Nikitin, A. V. Orphal, J., Perevalov, V., Perrin, A., Polovtseva, E. R., Richard, C., Smith, M. A. H., Starikova, E., Sung, K., Tashkun, S., Tennyson, J., Toon, G. C., Tyuterev, V. G., and Wagner, G.: The HITRAN2012 molecular spectroscopic database, *J. Quant. Spectrosc. Ra.*, 130, 4–50, 2013. 7

Schwartz, M. J., Read, W. G., and Van Snyder, W.: EOS MLS forward model polarized radiative transfer for Zeeman-split oxygen lines, *IEEE T. Geosci. Remote*, 44, 1182–1191, 2006. 3

Shvetsov, A. A., Fedoseev, L. I., Karashtin, D. A., Bol'shakov, O. S., Mukhin, D. N., Skalyga, N. K., and Feigin, A. M.: Measurement of the middle-atmosphere temperature profile using a groundbased spectroradiometer facility, *Radiophys. Quantum El.*, 53, 321–325, 2010. 3

Stähli, O., Murk, A., Kämpfer, N., Mätzler, C., and Eriksson, P.: Microwave radiometer to retrieve temperature profiles from the surface to the stratopause, *Atmos. Meas. Tech.*, 6, 2477–2494, doi:10.5194/amt-6-2477-2013, 2013. 3, 4, 5, 6

von Engeln, A. and Buehler, S. A.: Temperature profile determination from microwave oxygen emissions in limb sounding geometry, *J. Geophys. Res.*, 107, ACL12.1–ACL12.15, doi:10.1029/2001JD001029, 2002. 3

von Engeln, A., Buehler, S. A., Langen, J., Wehr, T., and Kuenzi, K.: Retrieval of upper stratospheric and mesospheric temperature profiles from millimeter-wave atmospheric sounder data, *J. Geophys. Res.*, 103, 31735–31748, 1998. 3

Zeeman, P.: On the influence of magnetism on the nature of the light emitted by a substance, *Astrophys. J.*, 5, 332–347, 1897. 6

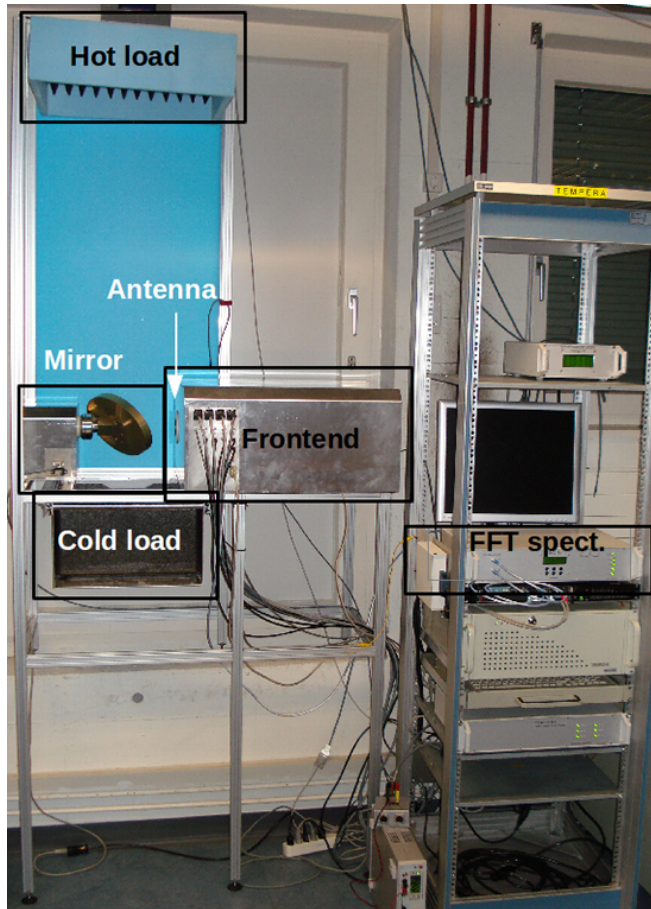


Figure 1. TEMPERA at the laboratory at ExWi, Bern (Switzerland).

AMTD

8, 1–32, 2015

Zeeman effect measurements in atmospheric O₂

F. Navas-Guzmán et al.

Title Page

Abstract

Introduction

Conclusions

References

Tables

Figures

◀

▶

◀

▶

Back

Close

Full Screen / Esc

Printer-friendly Version

Interactive Discussion



Zeeman effect measurements in atmospheric O₂

F. Navas-Guzmán et al.

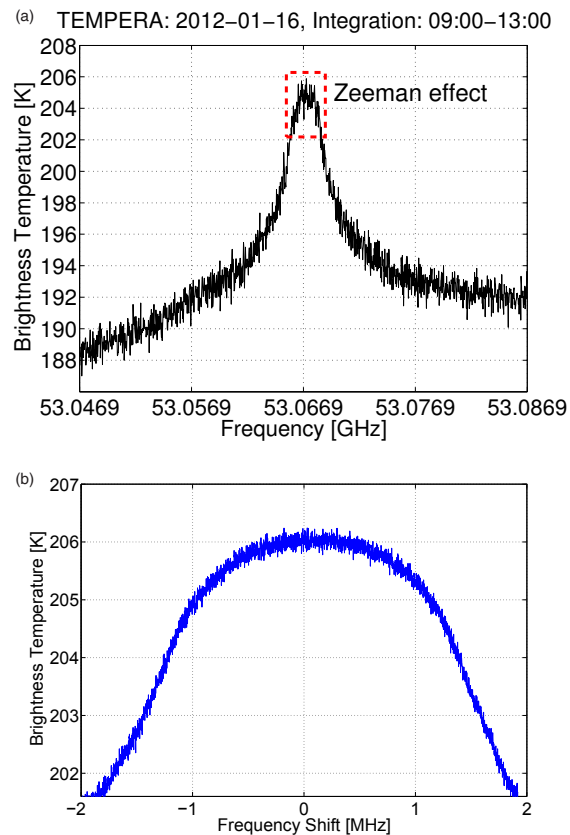


Figure 2. (a) Brightness temperature spectrum measured with the FFT spectrometer in the oxygen emission line of 53.07 GHz. The red box indicates the broadened line shape due to the Zeeman effect. (b) Monthly mean brightness temperature spectrum measured with the SDR spectrometer.

[Title Page](#)[Abstract](#)[Introduction](#)[Conclusions](#)[References](#)[Tables](#)[Figures](#)[◀](#)[▶](#)[◀](#)[▶](#)[Back](#)[Close](#)[Full Screen / Esc](#)[Printer-friendly Version](#)[Interactive Discussion](#)



Figure 3. Secondary mirror installed on the roof of the ExWi Building at the University of Bern.

AMTD

8, 1–32, 2015

Zeeman effect measurements in atmospheric O₂

F. Navas-Guzmán et al.

Title Page

Abstract

Introduction

Conclusions

References

Tables

Figures

◀

▶

◀

▶

Back

Close

Full Screen / Esc

Printer-friendly Version

Interactive Discussion



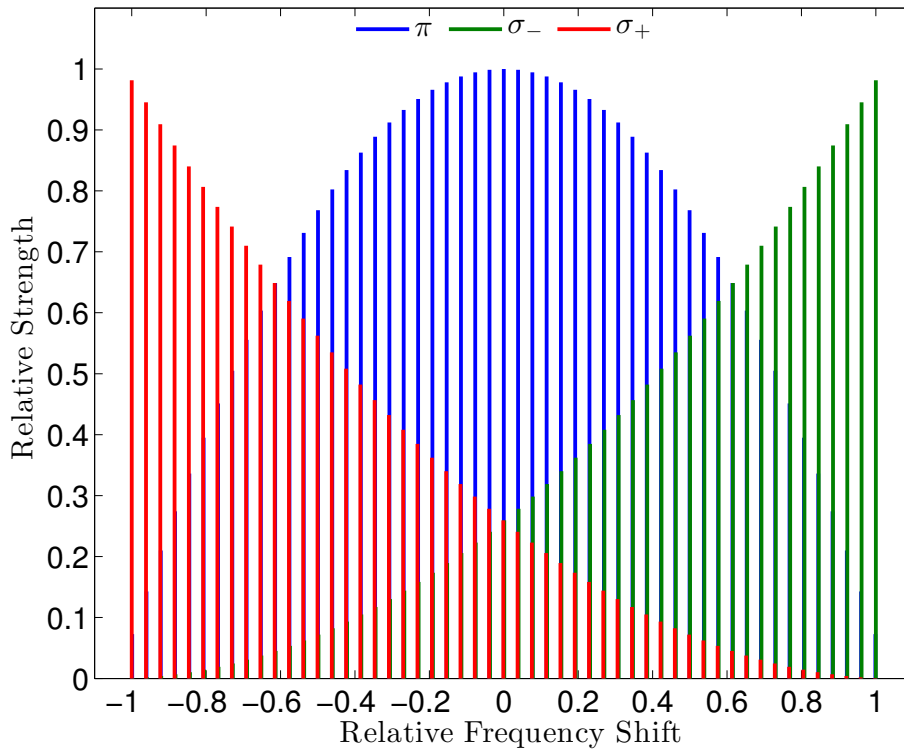


Figure 4. Example of Zeeman pattern for the 53 GHz $^{16}\text{O}_2$ line that is observed by TEMPERA. The colors represent the Zeeman component as indicated by the legend. The plot is renormalized on both axis as described in the text.

Zeeman effect measurements in atmospheric O_2

F. Navas-Guzmán et al.

Title Page	
Abstract	Introduction
Conclusions	References
Tables	Figures
◀	▶
◀	▶
Back	Close
Full Screen / Esc	
Printer-friendly Version	
Interactive Discussion	



Zeeman effect measurements in atmospheric O₂

F. Navas-Guzmán et al.

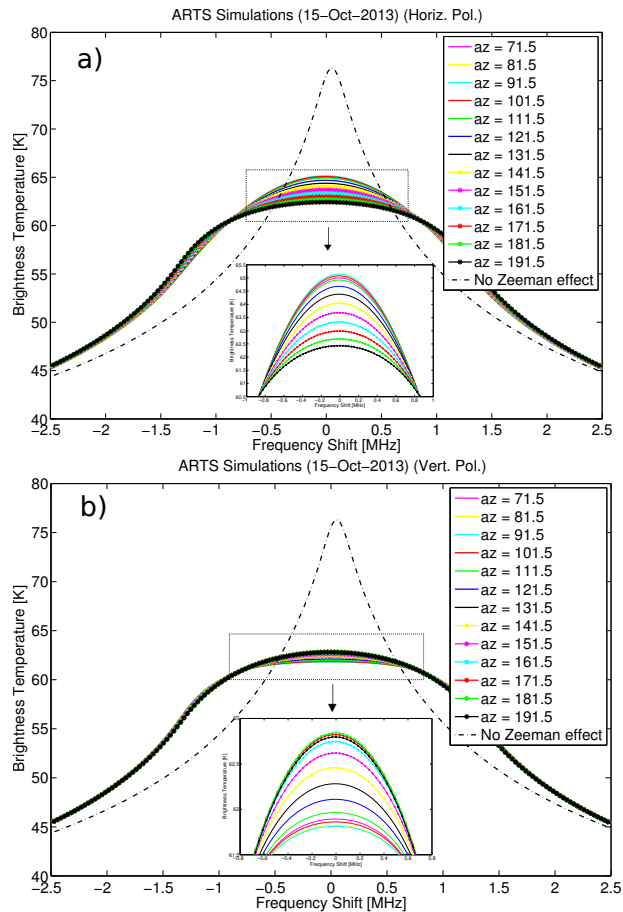


Figure 5. (a) Simulated horizontally polarized spectra on 15 October 2013 with (continuous lines) and without (dashed line) including the Zeeman effect. (b) As in (a) but considering vertical polarization.

[Title Page](#)
[Abstract](#)
[Introduction](#)
[Conclusions](#)
[References](#)
[Tables](#)
[Figures](#)
[Back](#)
[Close](#)
[Full Screen / Esc](#)
[Printer-friendly Version](#)
[Interactive Discussion](#)

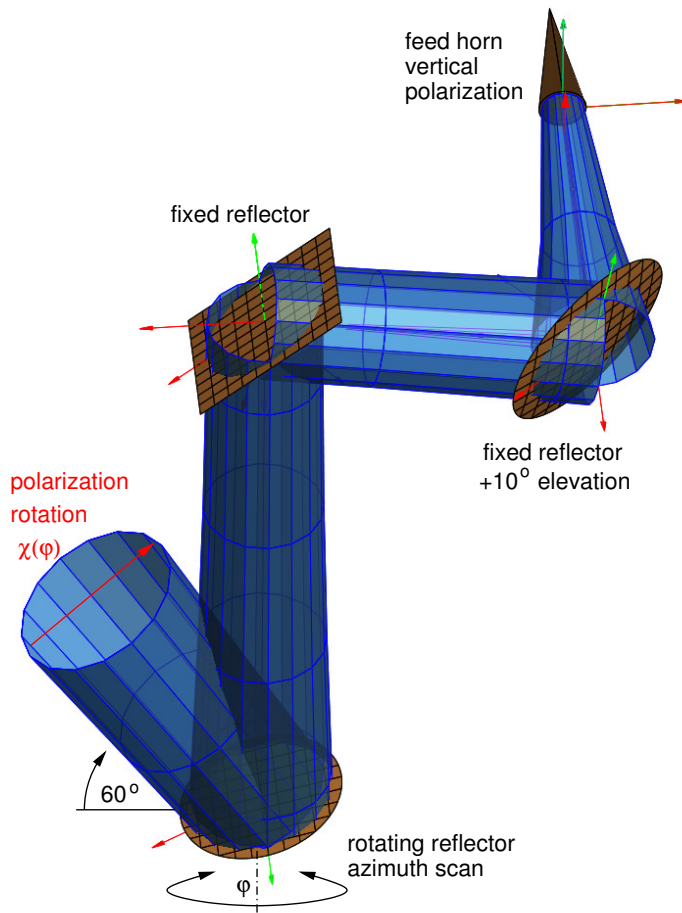


Figure 6. Simulation of the propagation of a vertical electric field from the TEMPERA antenna to the atmosphere and passing through the different mirrors using the GRASP package software.

Zeeman effect measurements in atmospheric O₂

F. Navas-Guzmán et al.

Title Page	
Abstract	Introduction
Conclusions	References
Tables	Figures
◀	▶
◀	▶
Back	Close
Full Screen / Esc	
Printer-friendly Version	
Interactive Discussion	



Zeeman effect measurements in atmospheric O₂

F. Navas-Guzmán et al.

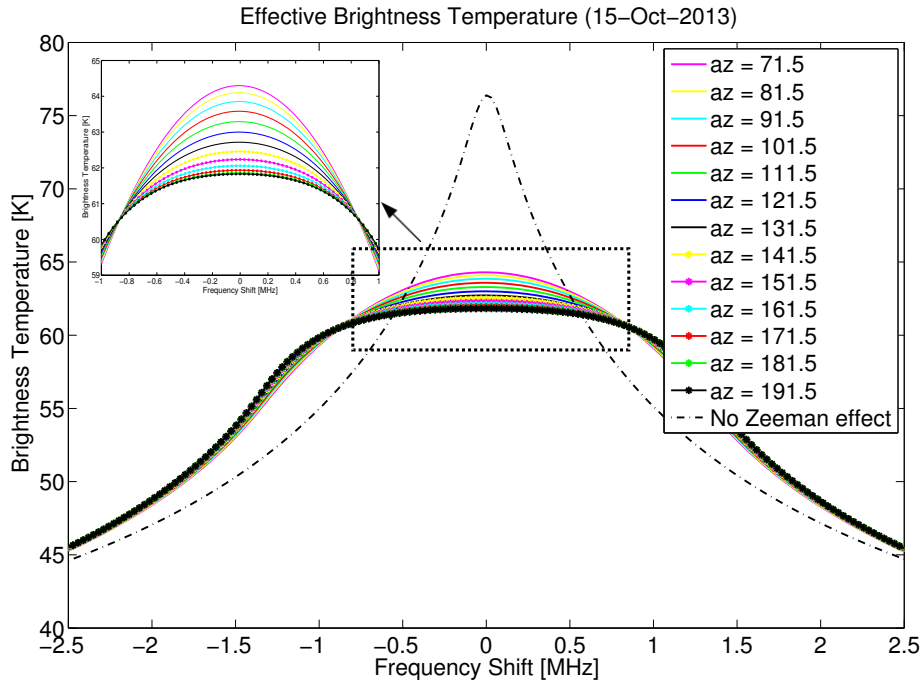


Figure 7. Simulated effective brightness temperature considering that the radiation passed through the different TEMPERA's components.

Title Page

Abstract

Introduction

Conclusions

References

Tables

Figures



Back

Close

Full Screen / Esc

Printer-friendly Version

Interactive Discussion



Zeeman effect measurements in atmospheric O₂

F. Navas-Guzmán et al.

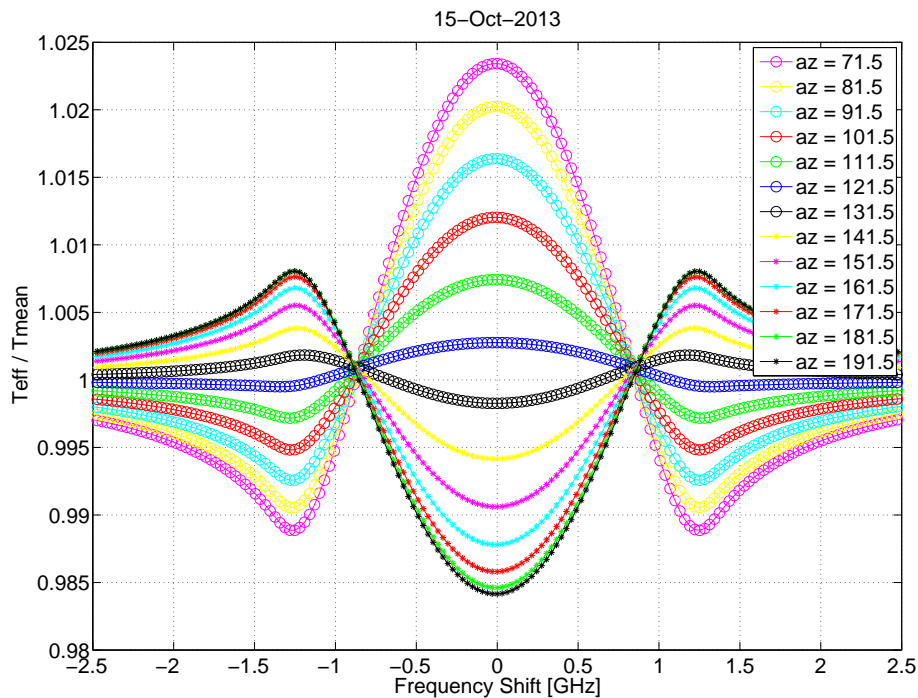


Figure 8. Ratio between the effective temperature for each observational angle and the averaged spectra for ARTS simulations.

[Title Page](#)[Abstract](#)[Introduction](#)[Conclusions](#)[References](#)[Tables](#)[Figures](#)[◀](#)[▶](#)[◀](#)[▶](#)[Back](#)[Close](#)[Full Screen / Esc](#)[Printer-friendly Version](#)[Interactive Discussion](#)

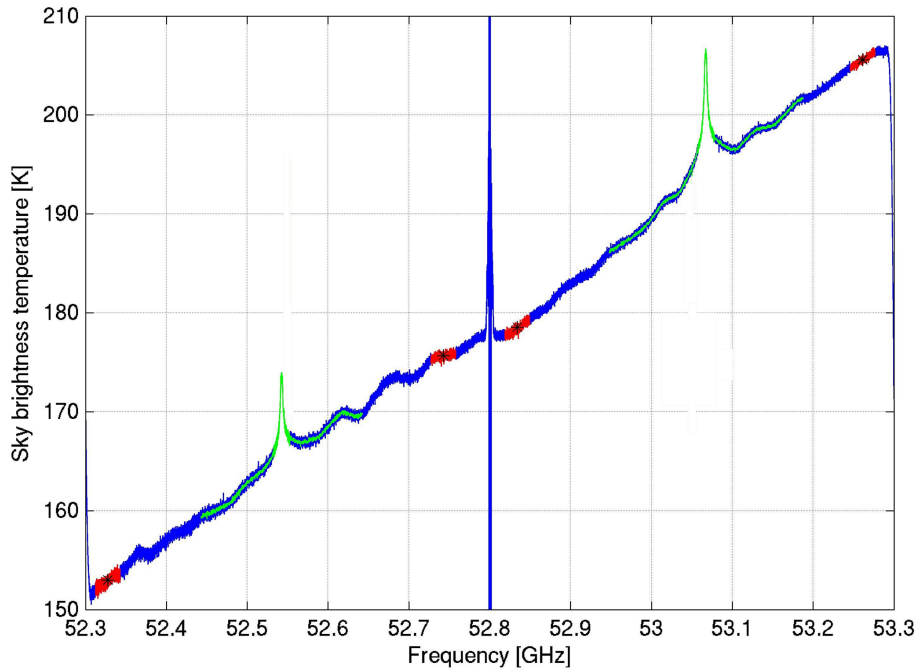


Figure 9. Example of calibrated spectrum of the FFT spectrometer. The frequency ranges marked in red are the areas used for the correction of tropospheric attenuation. The mean value of each range, indicated by a black star is the value used for the correction.

Zeeman effect measurements in atmospheric O₂

F. Navas-Guzmán et al.

Title Page	
Abstract	Introduction
Conclusions	References
Tables	Figures
◀	▶
◀	▶
Back	Close
Full Screen / Esc	
Printer-friendly Version	
Interactive Discussion	



